10/11/6/95 JSD

SLAC-PUB-95-7014
August 1995

CONF9509227--3

Bunch Compression at the Stanford Linear Collider*

R.L. Holtzapple, F.-J. Decker, and C. Simopoulos

Stanford Linear Accelerator Center, Stanford University, Stanford, California 94309

Abstract. The production and measurement of short electron and positron bunches in the Stanford Linear Collider (SLC) will be presented in this paper. The bunches are compressed in a transport line between the damping rings and the linac. The electron and positron bunch distributions in the SLC linac have been measured using a Hamamatsu, model N3373-02, 500-femtosecond streak camera [1]. The distributions were measured at the end of the SLC linac versus the bunch compressor RF voltage. The measurements are compared with simulations.

SLC BUNCH COMPRESSOR

The electron and positron bunch length extracted from the damping ring is too large (~5-7mm) for acceleration in a S-band accelerating structure, so the bunches must be compressed. There are two bunch compressors at the SLC, one for positrons and one for electrons. They are both located in the transport line from the damping rings to the linac.

The bunch compressor consists of two parts, the first part is an RF accelerating section located just after the exit of the damping ring, and the second part is a nonisochronous transport section after the accelerating section.

The longitudinal phase space of the extracted bunch from the damping ring is shown in figure 1a. After the damping ring, the bunch enters the RF accelerating section. The RF accelerating section is phased such that the bunch is on the zero crossing of the RF wave, so there is no overall acceleration. The phase is chosen to give the head of the bunch an energy gain while the tail of the bunch is decelerated. The RF section gives the bunch a correlated energy spread (figure 1b). Following the accelerating section the bunch is bent through a transport line with a positive momentum compaction of α_{comp}. Because of their higher energy the particles in the head of the bunch will travel over a longer path than the particles at the center of the bunch. The particles in the tail of the bunch will travel over a shorter distance than the center particles with a net result of a compressed bunch. The degree of compression (rotation in phase space) depends upon the amplitude of the RF voltage and the energy spread of the beam exiting the damping ring. The amplitude of the voltage can be adjusted to give a fully compressed (figure 1c), an under compressed (figure 1d) or an over compressed bunch (figure 1e) [2].

Presented at *Micro Bunches: A Workshop on the Production, Measurement and Applications of Short Bunches of Electrons and Positrons in Linacs and Storage Rings*, Upton, L.I., New York, September 28-30, 1995.

* Work supported by the Department of Energy contract DE-AC03-76SF00515.

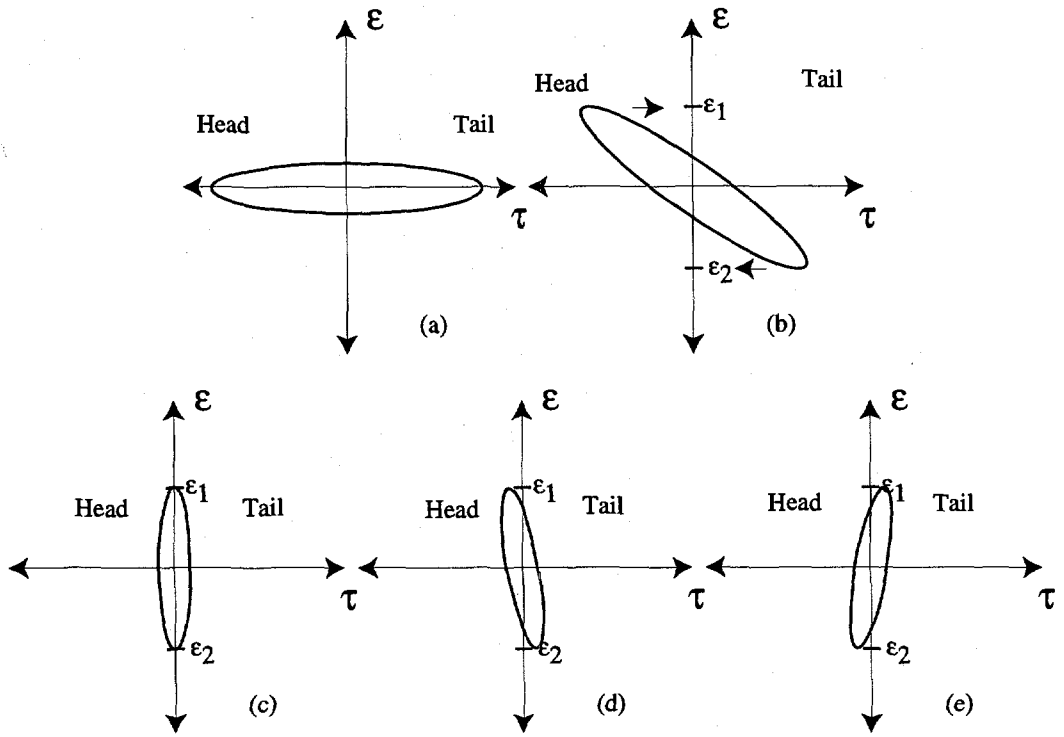

Figure 1. (a) The longitudinal phase space of the beam entering the RF accelerating section, (b) after the RF accelerating section, (c) entering the linac fully compressed, (d) under compressed, (e) and over compressed.

Following is a more quantitative discussion of the method of compression [3]. If the Gaussian energy spread and bunch length coming out of the damping ring are σ_ε and σ_τ the equation for a phase ellipse in longitudinal phase space is

$$\sigma_{\varepsilon_0}^2 \tau^2 + \sigma_{\tau_0}^2 \varepsilon^2 = \varepsilon_{l_i}^2 \tag{1}$$

where τ is the distance of the particle from the center of the bunch in units of time, ε is the energy deviation of the particle, and ε_{l_i} is the initial longitudinal emittance. After the damping ring the bunch goes through the compressor accelerating section and each particle's energy will be changed by an amount

$$\Delta E_{rf} = eV_{rf} \sin\left(\omega_{rf} \tau\right) \tag{2}$$

where ω_{rf} is the RF frequency, and eV_{rf} is the compressor voltage. For the following discussion

$$\Delta E_{rf} \approx \gamma\tau \quad \text{where} \quad \gamma = eV_{rf}\omega_{rf} \tag{3}$$

is used. The energy of each particle is changed depending upon its location in the bunch, and the energy deviation after the acceleration section is $\varepsilon \rightarrow \varepsilon + \Delta E_{rf}$. Substituting the energy deviation into the equation of the ellipse gives

$$\left(\sigma_{\varepsilon_0}^2 + \sigma_{\tau_0}^2 \gamma^2\right)\tau^2 + \sigma_{\tau_0}^2 \varepsilon^2 + 2\sigma_{\tau_0}^2 \gamma\tau\varepsilon = \varepsilon_{l_f}^2 \tag{4}$$

DISCLAIMER

Portions of this document may be illegible electronic image products. Images are produced from the best available original document.

where ε_{l_f} is the final longitudinal emittance.

After the acceleration section the bunch travels through the transport line. The transport line has a momentum compaction factor of α_{comp} and length L. The travel time difference from a particle with the ideal momentum, P_0, is given by $\Delta\tau = \frac{\Delta s}{c}$ where Δs is the change in the path length. The time shift in position through the transport line can be expressed in terms of the momentum compaction factor as

$$\Delta\tau = \frac{\alpha_{comp} L \varepsilon}{P_0 c^2} = \beta\varepsilon \quad \text{where} \quad \beta = \frac{\alpha_{comp} L}{P_0 c^2} . \tag{5}$$

The shift in time is $\tau \rightarrow \tau - \beta\varepsilon$ and substituting it into the phase ellipse equation gives

$$\begin{aligned} &\left(\sigma_{\varepsilon_0}^2 + \sigma_{\tau_0}^2\gamma^2\right)\tau^2 + 2\left(\sigma_{\tau_0}^2\left(\gamma - \beta\gamma^2\right) - \beta\sigma_{\varepsilon_0}^2\right)\varepsilon\tau \\ &+\left(\sigma_{\tau_0}^2(1-\gamma\beta)^2 + \sigma_{\varepsilon_0}^2\beta^2\right)\varepsilon^2 = \varepsilon_{l_f}^2 . \end{aligned} \tag{6}$$

The bunch length and energy spread after the bunch compressor are

$$\sigma_{\tau f} = \sqrt{\sigma_{\tau_0}^2\left(1 - \left(\frac{L\alpha_{comp}}{P_0 c}\right)\left(eV_{rf}\frac{2\pi}{\lambda_{rf}}\right)\right)^2 + \left(\frac{L\alpha_{comp}}{P_0 c^2}\right)^2 \sigma_{\varepsilon_0}^2} \tag{7}$$

$$\text{and } \sigma_{\varepsilon_f} = \sqrt{\sigma_{\varepsilon_0}^2 + \left(eV_{rf}\frac{2\pi}{\lambda_{rf}}\right)^2 \sigma_{z_0}^2} . \tag{8}$$

The longitudinal emittance entering the linac when the bunch length is minimized is $\varepsilon_{l_f} = \sigma_\varepsilon\sigma_\tau = \sigma_{\varepsilon_0}\sigma_{\tau_0} = \varepsilon_{l_i}$. The initial longitudinal emittance is equal to the final emittance as required by Liouville's theorem which states that the longitudinal phase space must be preserved for conservative forces.

The bunch length and energy spread can be plotted versus the RF voltage to illustrate the effects of the initial beam parameters on the final bunch distribution.

From figure 2a, several interesting features are evident:

1) The minimum bunch length is dependent on the initial energy spread and is given by $\sigma_\tau = \left(\frac{L\alpha_{comp}}{cP_0}\right)\sigma_{\varepsilon_0}$.

2) Away from the minimum, the bunch length is determined by the initial bunch length, and the final bunch length is not dependent upon the initial energy spread in this regime.

DISCLAIMER

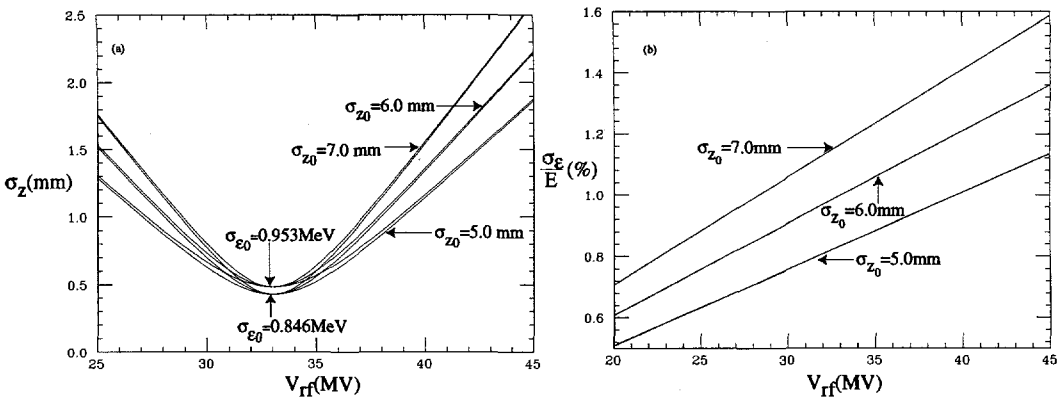

Figure 2. (a) The bunch length versus RF voltage for various initial bunch lengths and energy spreads for the SLC bunch compressor. (b) The energy spread of the beam entering the linac as a function of the RF voltage.

The final energy spread is plotted versus RF voltage for different initial values of bunch length and energy spread. As evident from figure 2b, the energy spread of the beam entering the linac is solely dependent upon the initial bunch length. For each bunch length two energy spread values (0.846 and 0.953 MeV) are plotted. The two values of energy spread overlap one another illustrating the independence of the final from the initial energy spread. The initial energy spread is determined by the damping ring and its equilibrium value is 0.846 MeV. A turbulent instability has been observed in the damping rings. When the current is raised the energy spread increases which will affect the minimum bunch length achieved in the linac [4].

The minimum bunch length occurs when the phase ellipse is up right, and the cross term in equation (6) is zero. The RF voltage necessary to minimize the bunch length is

$$eV_{rf} = \frac{1}{\omega_{rf}}\left(\frac{P_0 c^2}{L\alpha}\right) \approx 33 \text{ MV} . \tag{9}$$

The minimum bunch length and corresponding energy spread is

$$\sigma_{\tau f} = \frac{\sigma_{\varepsilon_0}}{eV_{rf}\omega_{rf}} \quad \text{and} \quad \sigma_{\varepsilon f} = eV_{rf}\sigma_{\tau_0}\omega_{rf} . \tag{10}$$

This section presented the longitudinal phase space changes in the compressor for a beam with a Gaussian distribution. In reality, the bunch distribution in the damping ring is not Gaussian due to potential well distortion and the effect of second order compression should also be included.

MEASUREMENT WITH STREAK CAMERA

The streak camera uses synchrotron light produced in the splitter magnet at the end of the linac to determine the longitudinal bunch distribution. The projections of the longitudinal distributions are saved and analyzed off-line.

The mean and σ of the projections are estimated by fitting the entire profile to an asymmetric Gaussian function [5]

$$I(z) = I_0 + I_1 \exp\left\{-\frac{1}{2}\left(\frac{(z-\bar{z})}{(1+sgn(z-\bar{z})A)\sigma}\right)^2\right\} \tag{11}$$

where I_0=pedestal, and I_1=peak of the asymmetric Gaussian. The term $sgn(z-\bar{z})A$ is the asymmetry factor which parameterizes the shape of the asymmetric Gaussian. Since the shape deviates from an asymmetric Gaussian, a better estimate of the bunch length is provided by the root mean square width

$$\sigma_z = \sqrt{\sum_i^N (z_i - \bar{z})^2 I(z_i)} \tag{12}$$

where N is the number of CCD pixels within $\pm 3\sigma$ of the mean $\bar{z}$, z_i is the location of the pixel, $I(z_i)$ is the projection height, and σ is determined by the fit.

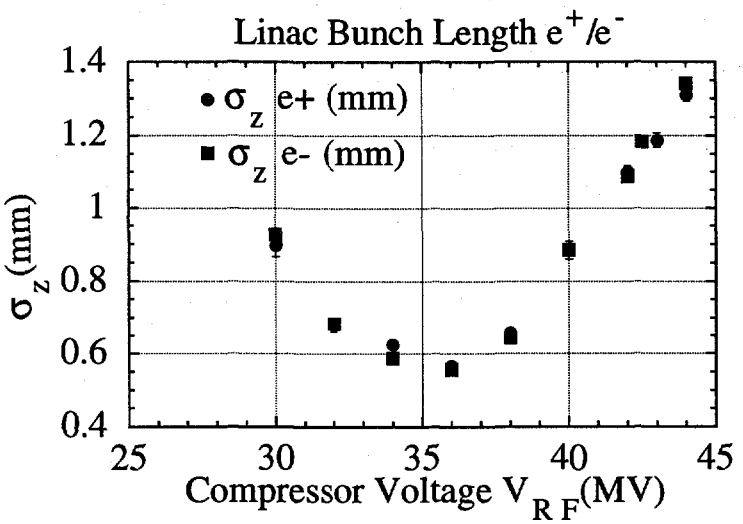

Figure 3. The bunch length as a function of the compressor voltage for the electron and positron bunch at the end of the linac.

The streak camera measurement consists of taking 30 longitudinal profiles at compressor voltage settings 2 MV apart. Plotted in figure 3 is the mean bunch length and the root mean error for currents of I=3.7x10^{10} and 3.3x10^{10} particles per bunch for the electrons and positrons respectively in the linac. The accelerating RF voltage in the damping rings during this measurement was 820 and 880 kV for the electron and positron rings respectively. The theoretical minimum bunch length is $\sigma_z = 0.56$ mm for the measured energy spread of $\frac{\sigma_E}{E} = 9x10^{-4}$. This minimum bunch length is in good agreement with the streak camera measurement.

A compressor voltage setting of 30 MV gives a bunch distribution that is under-compressed, 36 MV is fully-compressed, and 42 MV gives an over-compressed distribution. The longitudinal distribution of the positrons and electrons (figure 4 a, b) is a sum of 30 plots where the mean of the distributions is shifted to a common origin.

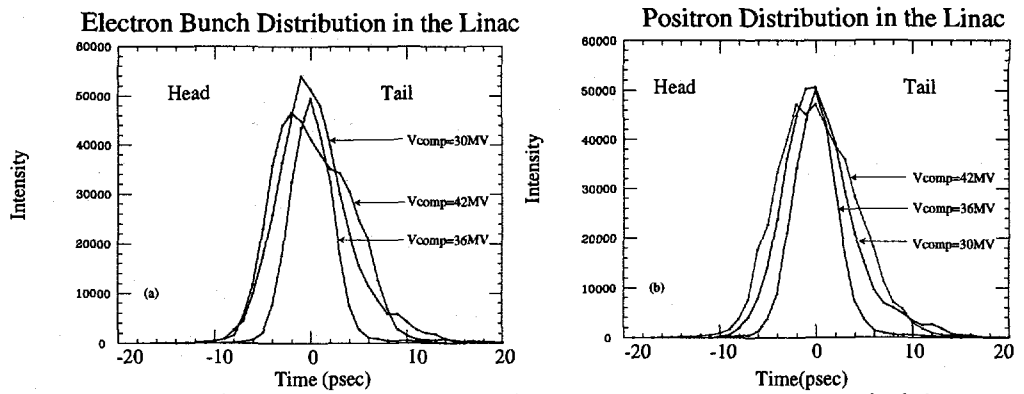

Figure 4. The (a) electron and (b) positron bunch distributions at the end of the linac for compressor voltage settings of 30, 36, and 42 MV.

The systematic errors addressed using the streak camera are: 1) dispersion in the light optics, 2) the slit width of the camera, and 3) the space charge effect at the photo cathode.

The dispersion in the glass optics limits the resolution of the streak camera as seen in figure 5(a). The effect of the dispersion can be minimized by using a narrow band (10nm FWHM) interference filter.

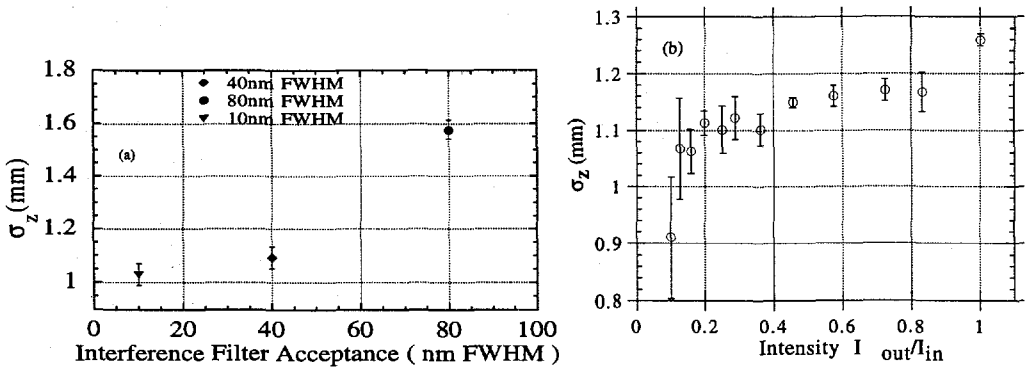

Figure 5. (a) The electron bunch length at the end of the linac as a function of interference filter acceptance. (b) The bunch length dependence on light intensity measured at the end of the linac with a current of $I=3.5\times10^{10}$.

To eliminate the intensity effects on the photo cathode, the multichannel plate gain was set to its maximum setting and the incident light was filtered until the bunch length measurement was stable over a range of light intensities. Figure 5(b) exhibits the intensity effects on bunch length measurement and in this example the light is filtered by 60% to eliminate this effect.

The slit width contributes to the resolution of the streak camera, by choosing 100 μm or less this contribution is negligible.

The ring to linac transport line beam pipe has a radius of $r = 2.25$ cm, and a peak dispersion of $\eta_x = 0.9$ m. This allows passage of particles that are ±2.5% within the mean energy of the bunch. The energy spread in the transport line determines the degree of compression. It is determined by the compressor's voltage. A linearized expression for the energy spread is

$$\frac{\sigma_E}{E} = 2\pi\left(\frac{\sigma_z}{\lambda E}\right)eV_{rf} \tag{13}$$

where σ_z is the damping ring bunch length, $\lambda = 105\text{mm}$ is the S-band wavelength, V_{rf} is the RF voltage amplitude, and E is the beam energy (1.19 GeV). During the 1994 run the compressor voltage amplitude was 43 MV and the bunch length out of the damping ring was $\sigma_z = 6.6$ mm. This results in an rms energy spread of 1.5% in the compressor transport line. The energy aperture in the transport line at the high dispersion regions is ±2.5% which results in current losses for the high and low energy tails.

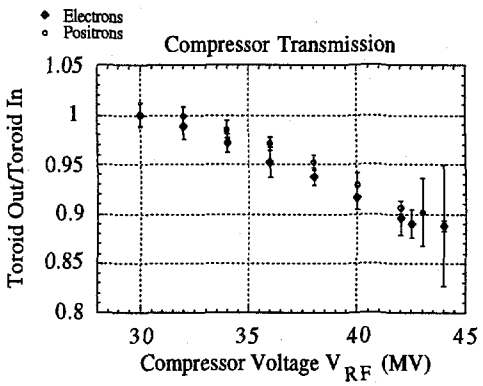

Figure 6. Electron and positron compressor transport line transmission as a function of compressor RF voltage.

Transmission through the positron and electron transport lines was measured versus compressor voltage with a toroid at the entrance and exit of the transport line. The ratio of the toroid readings (figure 6) determines the current loss. An over-compressed bunch results in a current loss of about 10% over an under-compressed bunch.

SIMULATION OF BUNCH COMPRESSOR BEAM DYNAMICS

The longitudinal beam dynamics simulated here begins with the bunch being extracted from the damping ring and then traveling through the bunch compressor.

The longitudinal phase space is initially determined by the damping rings. The energy distribution of a bunch in the damping ring is Gaussian and the bunch distribution can be described by an asymmetric Gaussian. The charge density expressed as an asymmetric Gaussian is given by equation (11) where A, I_1, and σ are the fitting parameters. For the following simulation 5000 particles are randomly generated according to the asymmetric Gaussian distribution. The initial damping ring bunch distribution (figure 7a, b) for a current of $I = 4.0x10^{10}$ has a measured rms of $\sigma = 6.6$ mm an asymmetry parameter of $A = 0.41$ and an energy spread of $\frac{\sigma_E}{E} = 9.0x10^{-4}$ [4]. A plot of the beam phase space before the compressor is shown in figure 8a.

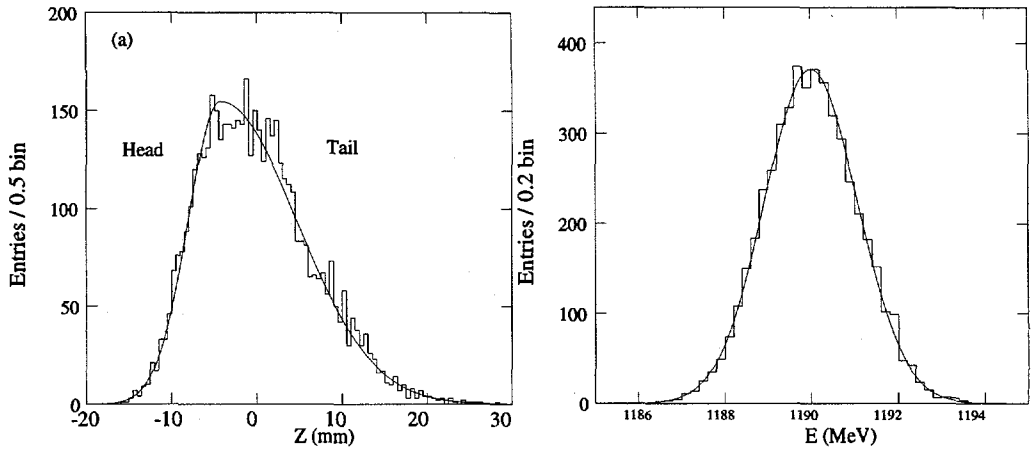

Figure 7. (a) A histogram of the bunch distribution described by an asymmetric Gaussian with $\sigma = 6.60$ mm and A=0.41. (b) A histogram of the energy distribution with an initial mean energy of $\langle E \rangle = 1190$ MeV and energy spread of $\frac{\sigma_E}{\langle E \rangle} = 9.0x10^{-4}$.

After the damping ring the bunch travels through the RF accelerating section where each particle will receive an energy gain given by equation (2). The phase space after the RF accelerating section is shown in figure 8b.

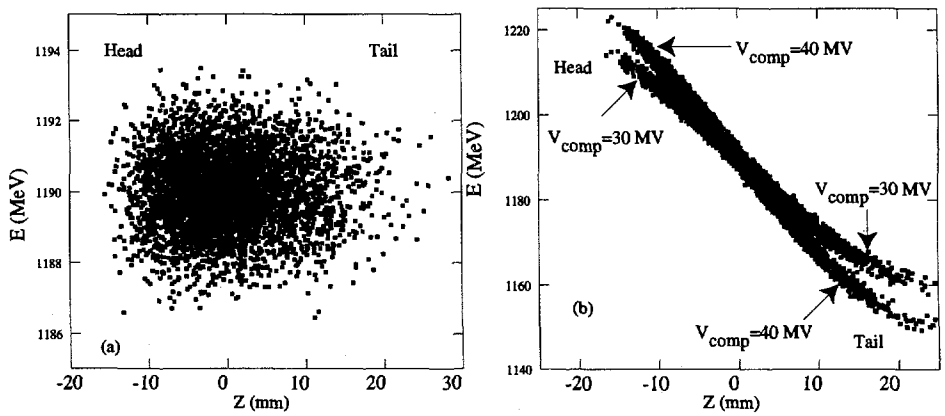

Figure 8. (a) The longitudinal phase space of the bunch after extraction from the damping ring. (b) The phase space of the bunch after the RF accelerating section for the compressor amplitudes of 30 and 40 MV.

The change in the longitudinal position for a particle is given by

$$z_f = z_i + R_{56}\left(\frac{E_i - \overline{E}}{\overline{E}}\right) + T_{566}\left(\frac{E_i - \overline{E}}{\overline{E}}\right)^2 \qquad (14)$$

where z_i, z_f are the initial and final longitudinal positions, $\overline{E}$ is the mean energy, E_i is the energy, $R_{56} = \alpha_{comp} L$, and $T_{566} = \frac{dR_{56}}{d\delta}$ for the transport line. Figure 9a shows the longitudinal phase space after the bunch compressor and three simulated bunch distributions are shown in figure 9b.

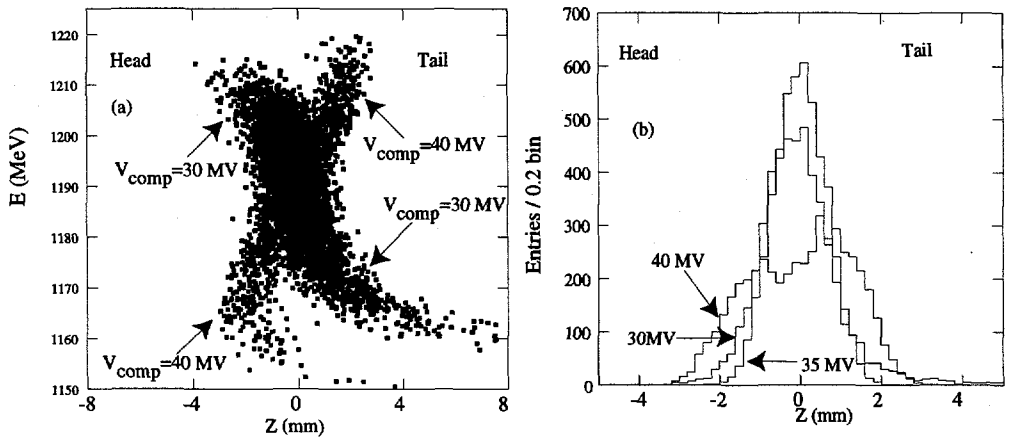

Figure 9. (a) The longitudinal phase space after the bunch compressor. (b) Histograms of the bunch distributions after the compressor.

Figure 10a is a plot of the simulated and measured bunch length as a function of voltage. The simulated bunch length is calculated using the same $\pm 3\sigma$ cut from the fit to an asymmetric Gaussian that was done with the streak camera images. The simulated and measured current transmission through the compressor line is plotted in figure 10b.

The simulation was done with two energy apertures. The design aperture is 2.5% and the aperture of 2.1% matches the measured transmission.

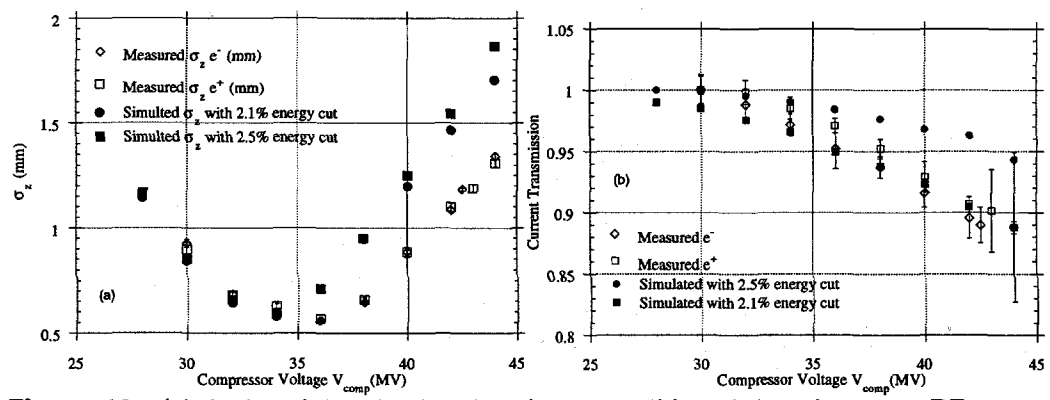

Figure 10. (a) A plot of the simulated and measured bunch length versus RF accelerating voltage. (b) The simulated and measured transmission loss in the compressor transport region.

SUMMARY

The measurements of the bunch distributions in the compressor transport line for positrons and electrons agree with each other. The simulations and measurements agree qualitatively, however the bunch length dependence on the RF voltage differs in the over compressed regime by 25%.

We checked the following possible reasons for the discrepancy. The RF calibration was checked and found to be linear (see figure 11). The initial

distribution was varied in the simulation for various σ and asymmetry factors. They were found to have a negligible effect.

Having excluded the above possibilities the higher order nonlinear terms in the arc optics need to be studied further.

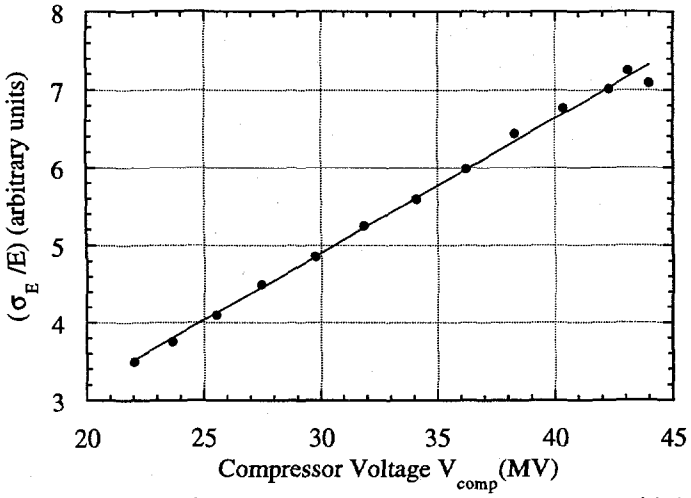

Figure 11. The energy spread measured with a wire scanner at a high dispersion region as a function of compressor voltage.

Acknowledgments

The authors would like to thank K. Jobe, P. Krejcik, M. Ross, R. Siemann, and D. Whittum for valuable discussions and helpful advice.

REFERENCES

[1] Hamamatsu Photonic Systems Corp., 360 Foothill Rd., Bridgewater, NJ 08807-6910.
[2] F.-J. Decker, R. Holtzapple, and T. Raubenheimer, "Over-Compression, a Method to Shape the Longitudinal Bunch Distribution for a Reduced Energy Spread", SLAC-PUB-6604, (1994).
[3] H. Wiedemann, "Bunchlength as a Function of the Compressor Voltage", SLAC CN# 117 (1981).
[4] R.L. Holtzapple, R.H. Siemann, and C. Simopoulos, "Measurement of Longitudinal Dynamics in the SLC Damping Rings", SLAC-PUB-95-6834, (1995).
[5] F.-J. Decker, "Beam Distribution Beyond RMS", SLAC-PUB-6684, (1994).